

Polycyclic polyprenylated acylphloroglucinol and phenolic metabolites from the aerial parts of *Hypericum elatoides* and their neuroprotective and anti-neuroinflammatory activities

Xi-Tao Yan^a, Zhen An^a, Yucui Huangfu^a, Yuan-Teng Zhang^a, Chun-Huan Li^a, Xin Chen^a,
Pei-Liang Liu^b, Jin-Ming Gao^{a,*}

^a Shaanxi Key Laboratory of Natural Products & Chemical Biology, College of Chemistry & Pharmacy, Northwest A&F University, Yangling 712100, People's Republic of China

^b Key Laboratory of Resource Biology and Biotechnology in Western China, College of Life Sciences, Northwest University, Xi'an 710069, People's Republic of China

ARTICLE INFO

Keywords:

Hypericum elatoides R. Keller
Hypericaceae
Polycyclic polyprenylated acylphloroglucinol
Flavanone-resveratrol adduct
Phenylpropanoid-substituted flavan-3-ol
Xanthone glycoside
Neuroprotective activity
Anti-neuroinflammatory activity

ABSTRACT

A phytochemical study on the aerial parts of *Hypericum elatoides* led to the isolation of a previously undescribed polycyclic polyprenylated acylphloroglucinol derivative, hyperelatone A, seven previously undescribed phenolic metabolites, hyperelatones B–H, along with ten known analogues. The structures of hyperelatones A–H were elucidated by 1D and 2D NMR spectroscopy, HRESIMS experiment, single-crystal X-ray diffraction and comparison of experimental and calculated ECD spectra, as well as chemical derivatization. All compounds were evaluated for their neuroprotective activity against hydrogen peroxide (H₂O₂)-induced cell injury in rat pheochromocytoma PC-12 cells and inhibitory effects on lipopolysaccharide (LPS)-induced nitric oxide (NO) production in BV-2 microglial cells. Hyperelatones B–D and H, cinchonain Ib, and tenuiside A showed noticeable neuroprotection at concentrations of 1.0–100.0 μM. Hyperelatones D, G, and H, (–)-epicatechin, tenuiside A, and (Z)-3-hexenyl-β-D-glucopyranoside exhibited significant anti-neuroinflammatory activity with IC₅₀ values ranging from 0.75 ± 0.02 to 5.83 ± 0.23 μM.

1. Introduction

The genus *Hypericum* belongs to the Hypericaceae family and comprises approximately 500 species of herbs, shrubs, and small trees, most of which are placed in temperate regions of the world (Crockett and Robson, 2011; Nürk et al., 2013). Previous phytochemical studies on *Hypericum* plants revealed the presence of polycyclic polyprenylated acylphloroglucinols (PPAPs) (Ciochina and Grossman, 2006; Yang et al., 2018), simple phloroglucinols (Zhao et al., 2015), xanthenes (Tanaka et al., 2009; Xu et al., 2016), flavonoids (Porzel et al., 2014), naphthodianthrones (Farag and Wessjohann, 2012), and benzophenones (Zhao et al., 2015) as major components. Many of them showed valuable biological activities, such as antidepressant (Grundmann et al., 2010; Jat, 2013), neuroprotective (Gómez del Rio et al., 2013; Zhou et al., 2016), memory-enhancing (Ben-Eliezer and Yechiam, 2016), cytotoxic (Zhao et al., 2015), anti-inflammatory (Huang et al., 2011), antimicrobial (Bridi et al., 2018), and antioxidant (Zheleva-Dimitrova et al., 2013) properties.

Hypericum elatoides R. Keller (Hypericaceae) is a perennial herb

grown as a narrow endemic species in Northwest China. Most recently, a series of uncommon biphenyl ether glycosides with remarkable neurotrophic activity have been isolated from *H. elatoides* (Yan et al., 2018). As part of our ongoing works to study the chemical diversity of *Hypericum* species and their beneficial biological activities for potential treatments of neurological disorders, the methanol extract of the aerial parts of *H. elatoides* were investigated. As a result, eight previously undescribed compounds, including a PPAP derivative (1), two flavanone-resveratrol adducts (2–3), a phenylpropanoid-substituted flavan-3-ol (4), and four xanthone glycosides (9–12), were isolated from *H. elatoides*, along with ten known compounds (5–8 and 13–18). We reported herein the isolation and structural elucidation of these previously undescribed compounds, as well as biological assessment of their neuroprotective effects against hydrogen peroxide (H₂O₂)-induced lesions of PC-12 cells and inhibitory effects on lipopolysaccharide (LPS)-induced nitric oxide (NO) production in BV-2 microglial cells.

* Corresponding author.

E-mail address: jinminggao@nwsuaf.edu.cn (J.-M. Gao).

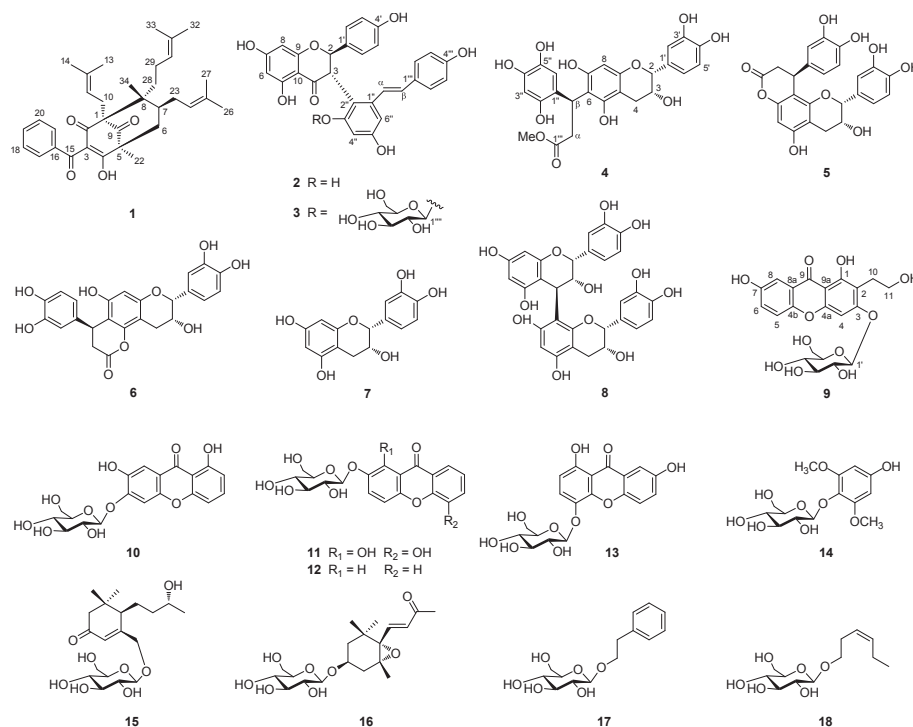


Fig. 1. Chemical structures of compounds 1–18.

2. Results and discussion

The crude MeOH extract of the aerial parts of *H. elatoides* was suspended in H₂O and partitioned successively with *n*-hexane, EtOAc, and *n*-BuOH. The obtained extracts were subjected to repeated column chromatography (CC) on silica gel, RP-C₁₈, and Sephadex LH-20 to afford eight previously undescribed compounds, hyperelatones A–H (1–4 and 9–12), and ten known analogues (5–8 and 13–18) (Fig. 1).

Hyperelatone A (1) was obtained as a colorless oil. Its molecular formula was determined to be C₃₄H₄₄O₄ by HRESIMS at *m/z* 517.3316 [M + H]⁺ (calcd for C₃₄H₄₅O₄, 517.3318), indicating 13 degrees of unsaturation. The IR spectrum showed absorption bands of hydroxy (3434 cm⁻¹) and carbonyl (1640 cm⁻¹) groups. The ¹H NMR spectrum (Table 1) exhibited resonances assignable to a monosubstituted benzene ring at δ_H 7.36–7.52 (5H, H-17–H-21), three trisubstituted olefins at δ_H 5.10 (1H, dd, *J* = 9.7, 1.4 Hz, H-11), 5.02 (1H, m, H-30), and 4.87 (1H, m, H-24), and eight methyl groups at δ_H 1.79, 1.69, 1.66, 1.66, 1.57, 1.50, 1.41, and 1.16 (each 3H, s, Me-14, 27, 13, 33, 32, 26, 22, and 34). Analysis of the ¹³C and DEPT NMR spectra implied that the structure of 1 possessed a bicyclo[3.3.1]nonane-2,4,9-trione core, based on the presence of an enolic β-diketone system at δ_C 194.1 (C-2), 115.5 (C-3), and 198.0 (C-4), a nonconjugated ketone at δ_C 208.8 (C-9), a methylene at δ_C 40.7 (C-6), a methine at δ_C 39.8 (C-7), and three quaternary carbons at δ_C 69.8 (C-1), 55.3 (C-5), and 51.2 (C-8) (Hamed et al., 2006; Acuña et al., 2010; Yang et al., 2015). The remaining carbon signals were assigned to a benzoyl group (including a carbonyl and six aromatic carbons), three prenyl groups (including six olefinic carbons, three methylenes, and six methyls), a methylene (C-28), and two methyl groups (Me-22 and Me-34). These observations suggested 1 to be a type-B bicyclic polyprenylated acylphloroglucinol derivative with a benzoyl group located at C-3 position (Yang et al., 2018). Its planar structure was established by the 2D NMR analysis (Fig. 2). ¹H–¹H COSY correlations of H-7 (δ_H 1.76)/H-23 (δ_H 2.05 and 1.96) and H-28 (δ_H 1.38 and 1.18)/H-29 (δ_H 1.86 and 1.79) as well as HMBC correlations from H-10 (δ_H 2.68 and 2.55) to C-1, C-2, C-8, and C-9 and from H-28 to C-1, C-7, and C-8 confirmed the connectivities of a 4-methyl-3-pentenyl to C-8 and two prenyl groups to C-1 and C-7,

respectively. Moreover, the attachments of two methyl groups at C-5 and C-8 were evidenced by the HMBC cross-peaks from Me-22 to C-4, C-5, C-6, and C-9 and from Me-34 to C-1, C-7, C-8, and C-28 (δ_C 35.9).

The relative configuration of 1 was elucidated via the NOESY spectrum, the key correlations of Me-22 (δ_H 1.41)/H-10b (δ_H 2.55), Me-22/H-6b (δ_H 1.99), H-6b/H-7 (δ_H 1.76), H-6b/H-28a (δ_H 1.18), and H-10b/H-28b (δ_H 1.38) indicated that H-7, CH₂-10, Me-22, and CH₂-28 were all α-oriented. The β-orientations for CH₂-23 and Me-34 were deduced from the NOESY correlations of Me-34 (δ_H 1.16)/H-23a (δ_H 1.96) and Me-34/H-10a (δ_H 2.68). In addition, a single-crystal X-ray diffraction pattern (CCDC 1875447) was acquired using Mo Kα radiation. The crystallography data of 1 further confirmed the planar structure and permitted unambiguous assignment of the absolute configuration as (1*S*,5*S*,7*S*,8*R*) with a Flack parameter of 0(2) (Fig. 2). Thus, the structure of 1, hyperelatone A, was elucidated as shown in Fig. 1.

Hyperelatone B (2) was obtained as a yellow amorphous powder. Its molecular formula was established as C₂₉H₂₂O₈ by HRESIMS (*m/z* 521.1221 [M + Na]⁺, calcd for C₂₉H₂₂NaO₈, 521.1212). The IR spectrum showed absorption bands at 3405 and 1635 cm⁻¹ for hydroxy and carbonyl groups, respectively. The ¹H NMR spectrum of 2 (Table 2) revealed the presence of two 1,4-disubstituted aromatic rings with AA'BB' coupling system [δ_H 7.19 (2H, d, *J* = 8.4 Hz, H-2'' and H-6'''), 7.00 (2H, d, *J* = 8.4 Hz, H-2' and H-6'), 6.74 (2H, d, *J* = 8.4 Hz, H-3'' and H-5'''), and 6.56 (2H, d, *J* = 8.4 Hz, H-3' and H-5')], a *trans*-olefinic moiety [δ_H 6.51 (1H, d, *J* = 15.8 Hz, H-α) and 6.34 (1H, d, *J* = 15.8 Hz, H-β)], and two 1,2,3,5-tetrasubstituted aromatic rings with the protons located at the *meta*-positions [δ_H 6.27 (1H, br s, H-6''), 6.24 (1H, br s, H-4''), and 5.92 (2H, overlap, H-6 and H-8)], which was supported by the HMBC correlations from the aromatic protons at δ_H 6.27 to C-2'' (δ_C 113.1) and C-4'' (δ_C 103.1), from δ_H 6.24 to C-2'' and C-6'' (δ_C 105.9), and from δ_H 5.92 to C-6 (δ_C 97.3), C-8 (δ_C 96.3), and C-10 (δ_C 103.4). The remaining proton signals were attributable to an oxymethine at δ_H 5.75 (1H, d, *J* = 11.7 Hz, H-2) and a methine with vicinal coupling at δ_H 4.35 (1H, d, *J* = 11.7 Hz, H-3), which was confirmed by the ¹H–¹H COSY correlation of H-2/H-3. The large coupling constant (*J* = 11.7 Hz) between H-2 and H-3 indicated their *trans*-

Table 1
NMR spectroscopic data for compound **1** at 500 MHz (^1H) and 125 MHz (^{13}C) in CDCl_3 .

Position	δ_{C} , type	δ_{H} , mult (J in Hz)	HMBC (H \rightarrow C)
1	69.8, C		
2	194.1, C		
3	115.5, C		
4	198.0, C		
5	55.3, C		
6	40.7, CH ₂	2.34, d (14.4) 1.99, dd (14.4, 7.0)	4, 5, 7, 8, 9, 22, 23 4, 5, 7, 9, 22, 23
7	39.8, CH	1.76, m	1, 5, 23, 24
8	51.2, C		
9	208.8, C		
10	26.2, CH ₂	2.68, dd (13.5, 9.7) 2.55, d (12.9)	1, 2, 8, 9, 11, 12 1, 2, 9, 11, 12
11	120.4, CH	5.10, dd (9.7, 1.4)	13, 14
12	135.1, C		
13	18.4, CH ₃	1.66, s	11, 12, 14
14	26.3, CH ₃	1.79, s	11, 12, 13
15	197.0, C		
16	137.1, C		
17	129.0, CH	7.52, d (8.0)	15, 19, 21
18	128.0, CH	7.36, t (8.0)	16, 20
19	132.7, CH	7.51, t, (7.8)	17, 21
20	128.0, CH	7.36, t, (8.0)	16, 18
21	129.0, CH	7.52, d (8.0)	15, 17, 19
22	17.6, CH ₃	1.41, s	4, 5, 6, 9
23	28.6, CH ₂	1.96, m 2.05, m	24, 25 24, 25
24	124.4, CH	4.87, m	26, 27
25	133.2, C		
26	18.0, CH ₃	1.50, s	24, 25, 27
27	26.0, CH ₃	1.69, s	24, 25, 26
28	35.9, CH ₂	1.18, m 1.38, m	1, 7, 8, 29, 30, 34 1, 7, 8, 29, 30, 34
29	22.7, CH ₂	1.79, m 1.86, m 5.02, m	28, 30, 31 28, 30, 31 28, 29, 32, 33
30	124.0, CH		
31	132.2, C		
32	17.8, CH ₃	1.57, s	30, 31, 33
33	25.9, CH ₃	1.66, s	30, 31, 32
34	18.8, CH ₃	1.16, s	1, 7, 8, 28

stereochemistry. The ^{13}C NMR and HSQC spectra of **2** showed signals for two methines at δ_{C} 83.3 (C-2) and 54.2 (C-3), a ketone at δ_{C} 200.2 (C-4), a double bond at δ_{C} 125.2 (C- α) and 132.5 (C- β), and 20 aromatic carbons at δ_{C} 96.3–167.9, four of which were double [δ_{C} 129.4 (C-2' and C-6'), 129.0 (C-2'' and C-6''), 116.5 (C-3'' and C-5''), and 115.6 (C-3' and C-5')], corresponding to two 1,4-disubstituted aromatic rings shown from ^1H NMR spectrum. The HMBC spectrum of **2** (Fig. 3) exhibited key correlations from H- α to C-1''' (δ_{C} 130.8), C-2'' (δ_{C} 113.1), and C-6'' (δ_{C} 105.9) and from H- β to C-1'' (δ_{C} 143.1), C-1'', C-2''', and C-6''', indicating the presence of a 3,5,4'-trihydroxystilbene (resveratrol) moiety. In addition, the HMBC correlations from H-2 to C-1' (δ_{C} 131.5), C-2' and C-6' and from H-3 to C-1', C-2, and C-4 indicated the presence

of a 4',5,7-trihydroxyflavanone (naringenin) moiety. The linkage between the naringenin unit and the resveratrol unit was determined to be C-3–C-2'' by analysis of the HMBC correlations from H-3 to C-1'', C-2'', and C-3'' (δ_{C} 157.4).

The absolute configurations at the chiral centers C-2 and C-3 were established by comparing the experimental and computed electronic circular dichroism (ECD) spectra. The ECD spectrum of **2** exhibited a strong positive Cotton effect near 291 nm ($\pi \rightarrow \pi^*$ transitions), in an opposite manner to struthiolanone (2*S*,3*R*) (Ayers et al., 2008), which was the first and only report of a flavanone-stilbene adduct, suggesting the absolute configuration of **2** as (2*R*,3*S*) (Jamila et al., 2014; Vu et al., 2016). This assignment was confirmed by computational calculations of the ECD spectra. The calculated ECD spectrum of the (2*R*,3*S*) isomer of **2** well matched the experimental one (Fig. 4). Based on these data, the structure of **2** was established as (2*R*,3*S*)-naringenin-(3*\alpha*,2)-*trans*-3,5,4'-trihydroxystilbene.

Hyperelatone C (**3**) was obtained as a yellow amorphous powder with a molecular formula of $\text{C}_{35}\text{H}_{32}\text{O}_{13}$, which was determined by HRESIMS at m/z 683.1760 $[\text{M} + \text{Na}]^+$ (calcd for $\text{C}_{35}\text{H}_{32}\text{NaO}_{13}$, 683.1741). The ^1H and ^{13}C NMR spectra of **3** showed similar resonance patterns to those found for **2** (Table 2), with an additional sugar moiety at δ_{H} 5.04 (1H, d, $J = 7.7$ Hz, H-1'''), 3.93 (1H, dd, $J = 11.9, 1.6$ Hz, H-6a'''), 3.72 (1H, dd, $J = 11.9, 5.7$ Hz, H-6b'''), 3.44 (2H, m, H-3'' and H-5'''), 3.33 (1H, m, H-4'''), and 3.24 (1H, m, H-2'''); δ_{C} 101.8 (C-1'''), 78.5 (C-5'''), 78.5 (C-3'''), 75.4 (C-2'''), 71.4 (C-4'''), and 62.8 (C-6'''). Acid hydrolysis followed by HPLC analysis after arylthiocarbamoyl-thiazolidine derivatization confirmed the characterization of a D-glucose and the coupling constant ($J = 7.7$ Hz) confirmed the β -anomer for the glucose moiety. The location of the β -D-glucopyranosyl unit was determined to be at C-3'' by analysis of the HMBC spectrum of **3**, which showed a correlation from the anomeric proton (H-1''') to C-3'' (δ_{C} 157.2) (Fig. 3). The *trans*-configuration of H-2 and H-3 was established by the large coupling constant ($J = 11.8$ Hz) between H-2 and H-3. The absolute stereochemistry of C-2 and C-3 was determined to be (2*R*,3*S*)-configuration based on the observed positive Cotton effect at 291 nm in the ECD spectrum of **3** (Fig. 4), in agreement with the ECD data of **2**. Thus, the structure of **3** was elucidated as (2*R*,3*S*)-naringenin-(3*\alpha*,2)-*trans*-5,4'-dihydroxystilbene-3-*O*- β -D-glucopyranoside.

Hyperelatone D (**4**) was obtained as a brown amorphous powder with a molecular formula of $\text{C}_{25}\text{H}_{24}\text{O}_{11}$, as inferred from the positive HRESIMS at m/z 482.1209 $[\text{M} - \text{H}_2\text{O}]^+$ (calcd for $\text{C}_{25}\text{H}_{22}\text{O}_{10}$, 482.1213). The IR absorptions indicated the presence of hydroxy (3436 cm^{-1}) and ester carbonyl (1642 cm^{-1}) groups. The ^1H NMR spectrum (Table 2) revealed the occurrence of a set of ABX coupled aromatic protons at δ_{H} 7.00 (1H, d, $J = 1.9$ Hz, H-2'), 6.87 (1H, dd, $J = 8.2, 1.9$ Hz, H-6'), and 6.80 (1H, d, $J = 8.2$ Hz, H-5'), a singlet aromatic proton at δ_{H} 6.13 (1H, s, H-8), two oxymethine at δ_{H} 4.93 (1H, br s, H-2) and 4.26 (1H, m, H-3), and a methylene at δ_{H} 2.93 (1H, dd, $J = 17.1, 4.5$ Hz, H-4a) and 2.84 (1H, dd, $J = 17.1, 2.3$ Hz, H-4b), suggesting the presence of an epicatechin skeleton in **4** (Davis et al.,

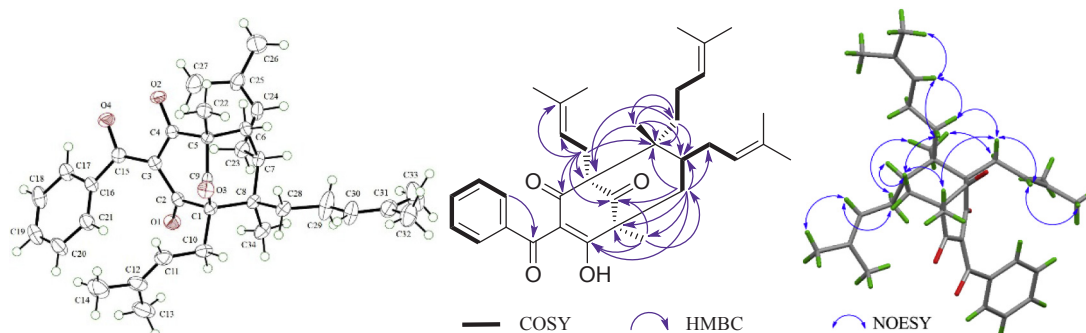


Fig. 2. ORTEP drawing and key ^1H - ^1H COSY, HMBC, and NOESY correlations of compound **1**.

Table 2
 ^1H NMR (500 MHz) and ^{13}C NMR (125 MHz) spectroscopic data for compounds 2–4 in CD_3OD .

Position	2		3		4	
	δ_{C} , tpye	δ_{H} , mult (J in Hz)	δ_{C} , tpye	δ_{H} , mult (J in Hz)	δ_{C} , tpye	δ_{H} , mult (J in Hz)
2	83.3, CH	5.75, d (11.7)	83.3, CH	5.84, d (11.8)	80.3, CH	4.93, br s
3	54.2, CH	4.35, d (11.7)	54.2, CH	4.46, d (11.8)	67.0, CH	4.26, m
4	200.2, C		199.7, C		29.6, CH_2	2.84, dd (17.1, 2.3) 2.93, dd (17.1, 4.5)
5	165.8, C		165.8, C		153.0, C	
6	97.3, CH	5.92, overlap	97.5, CH	5.92, br s	104.7, C	
7	167.9, C		168.1, C		153.6, C	
8	96.3, CH	5.92, overlap	96.3, CH	5.92, br s	96.0, CH	6.13, s
9	165.0, C		165.0, C		156.7, C	
10	103.4, C		103.4, C		103.3, C	
1'	131.5, C		131.3, C		132.3, C	
2'	129.4, CH	7.00, d (8.4)	129.6, CH	7.05, d (8.4)	115.4, CH	7.00, d (1.9)
3'	115.6, CH	6.56, d (8.4)	115.6, CH	6.54, d (8.4)	146.0, C	
4'	158.6, C		158.5, C		146.3, C	
5'	115.6, CH	6.56, d (8.4)	115.6, CH	6.54, d (8.4)	116.2, CH	6.80, d (8.2)
6'	129.4, CH	7.00, d (8.4)	129.6, CH	7.05, d (8.4)	119.4, CH	6.87, dd (8.2, 1.9)
1''	143.1, C		143.5, C		116.1, C	
2''	113.1, C		114.7, C		146.7, C	
3''	157.4, C		157.2, C		104.5, CH	6.47, s
4''	103.1, CH	6.24, br s	102.5, CH	6.61, d (1.9)	142.3, C	
5''	158.4, C		158.4, C		146.1, C	
6''	105.9, CH	6.27, br s	108.4, CH	6.42, d (1.9)	115.3, CH	6.63, s
α	125.2, CH	6.51, d (15.8)	124.7, CH	6.57, d (15.9)	44.9, CH_2	2.51, dd (14.6, 8.9) 2.98, dd (14.6, 3.6)
β	132.5, CH	6.34, d (15.8)	133.3, CH	6.33, d (15.9)	31.4, CH	4.49, dd (8.9, 3.6)
1'''	130.8, C		130.6, C		174.8, C	
2'''	129.0, CH	7.19, d (8.4)	129.2, CH	7.21, d (8.5)	52.2, CH_3	3.60, s
3'''	116.5, CH	6.74, d (8.4)	116.5, CH	6.75, d (8.5)		
4'''	158.5, C		158.9, C			
5'''	116.5, CH	6.74, d (8.4)	116.5, CH	6.75, d (8.5)		
6'''	129.0, CH	7.19, d (8.4)	129.2, CH	7.21, d (8.5)		
1''''			101.8, CH	5.04, d (7.7)		
2''''			75.4, CH	3.24, m		
3''''			78.5, CH	3.44, m		
4''''			71.4, CH	3.33, m		
5''''			78.5, CH	3.44, m		
6''''			62.8, CH_2	3.72, dd (11.9, 5.7) 3.93, dd (11.9, 1.6)		

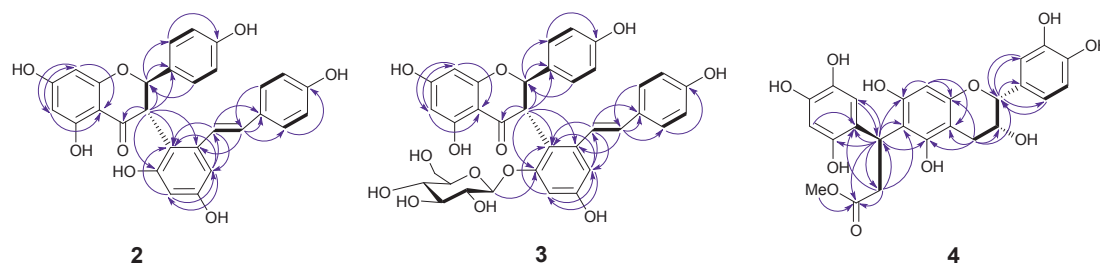


Fig. 3. Key ^1H - ^1H COSY (bold lines) and HMBC (\rightarrow) correlations of compounds 2–4.

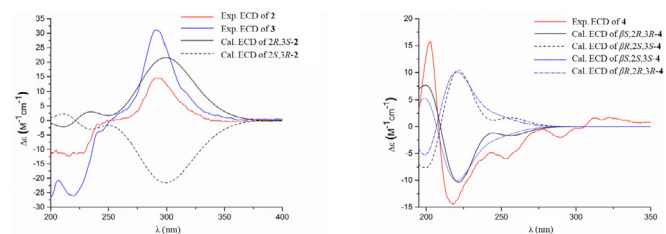


Fig. 4. Experimental ECD spectra of compounds 2–4 and their calculated ECD spectra at the B3LYP/6-31 + G(d,p) level in MeOH.

1996; Abd El-Razek, 2007). Moreover, the characteristic epicatechin carbons at δ_{C} 80.3 (C-2), 67.0 (C-3), and 29.6 (C-4) were also present in the ^{13}C NMR spectrum. The remaining proton signals were assigned to a

1,2,4,5-tetrasubstituted aromatic ring with two protons located at the *para*-position [δ_{H} 6.63 (1H, s, H-6'') and 6.47 (1H, s, H-3'')], a benzylic methine [δ_{H} 4.49 (1H, dd, $J = 8.9, 3.6$ Hz, H- β)], a methylene [δ_{H} 2.98 (1H, dd, $J = 14.6, 3.6$ Hz, H- $\alpha\alpha$) and 2.51 (1H, dd, $J = 14.6, 8.9$ Hz, H- $\alpha\beta$)], and a methoxy group [δ_{H} 3.60 (3H, s, H-2''')]. The ^{13}C NMR spectrum of 4 exhibited ten additional carbon signals comprising one ester carbonyl (δ_{C} 174.8), six aromatic carbons (δ_{C} 146.7, 146.1, 142.3, 116.1, 115.3, and 104.5), one methoxy carbon (δ_{C} 52.2), and two aliphatic carbons (δ_{C} 44.9 and 31.4). These data indicated the presence of a β -substituted phenylpropanoate unit (Foo, 1987; Lee et al., 2001). Complete assignment of the ^1H and ^{13}C NMR signals of 4 was accomplished by analysis of 2D NMR spectra (Fig. 3) and by comparison with those published NMR spectroscopic data of several phenylpropanoid-substituted catechins (Tang et al., 2007; Huang et al., 2007; Zhang et al., 2013). Most importantly, the key HMBC correlations from H- β to

C-5 (δ_C 153.0), C-6 (δ_C 104.7), and C-7 (δ_C 153.6), from H- α to C-6, from H-4 to C-5, C-9 (δ_C 156.7), and C-10 (δ_C 103.3), and from H-8 to C-9 indicated that the phenylpropanoate unit was connected to the epicatechin skeleton via the linkage of C- β -C-6.

The *cis*-configuration of H-2 and H-3 was deduced by the evidence of a broad singlet signal due to H-2, suggesting a negligible coupling constant between H-2 and H-3. The absolute configuration of the C- β stereogenic center was determined via comparison of the experimental ECD spectrum of **4** with the calculated ECD spectra of the (βS ,2*R*,3*R*), (βR ,2*S*,3*S*), (βS ,2*S*,3*S*), and (βR ,2*R*,3*R*) enantiomers (Fig. 4). The experimental ECD spectrum of **4** showed a strong negative Cotton effect at 218 nm, consistent with the calculated curves of (βS) enantiomers [(βS ,2*R*,3*R*)-**4** and (βS ,2*S*,3*S*)-**4**], allowing assignment of the (βS) absolute configuration. Moreover, the (βS ,2*R*,3*R*)-**4** showed the best match. Considering the isolation of a large amount of (–)-epicatechin (2*R*,3*R*) (**7**, 1341.4 mg) and its derivatives (**5**, **6**, and **8**) from *H. elatoides*, they are likely to be products of the same biosynthetic pathway, and therefore the absolute stereochemistry of C-2 and C-3 can be assumed to be (2*R*,3*R*), which was also supported by the chemical shifts of C-ring (Abd El-Razek, 2007). Accordingly, the absolute configuration of **4** was deduced to be (βS ,2*R*,3*R*). The structure of **4** was proposed as 6-[(1*S*)-(2,4,5-trihydroxyphenyl)-3-methoxy-3-oxopropyl]-epicatechin.

Hyperelatone E (**9**) was obtained as a yellow amorphous powder that analyzed for C₂₁H₂₂O₁₁ by HRESIMS (*m/z* 451.1233 [M + H]⁺, calcd for C₂₁H₂₂O₁₁, 451.1240), accounting for 11 degrees of unsaturation. The IR spectrum displayed absorption bands due to hydroxy (3414 cm⁻¹) and conjugated carbonyl (1706 cm⁻¹) groups. The ¹H NMR data of **9** showed the presence of two hydroxy groups at δ_H 13.10 (1H, s, 1-OH) and 10.06 (1H, s, 7-OH), a group of ABX coupled aromatic protons at δ_H 7.53 (1H, d, *J* = 9.0 Hz, H-5), 7.44 (1H, d, *J* = 2.7 Hz, H-8), and 7.32 (1H, dd, *J* = 9.0, 2.7 Hz, H-6), a singlet aromatic proton at δ_H 6.77 (1H, s, H-4), an anomeric proton at δ_H 5.05 (1H, d, *J* = 6.9 Hz, H-1'), and a hydroxyethyl moiety contributed by a hydroxy signal at δ_H

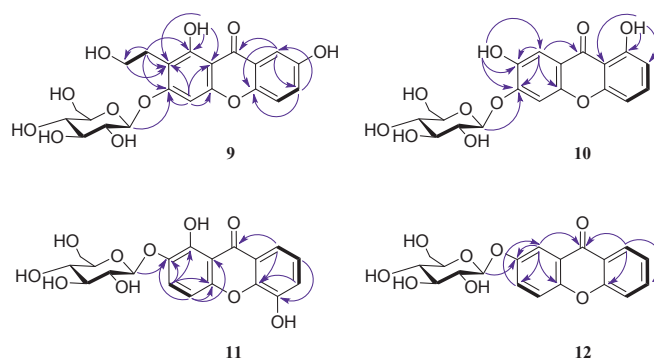


Fig. 5. Key ¹H-¹H COSY (bold lines) and HMBC (→) correlations of compounds **9**–**12**.

4.60 (1H, t, *J* = 5.5 Hz, 11-OH) and two methylene signals at δ_H 2.87 and 2.80 (each 1H, m, H-10) and 3.51 (2H, m, H-11) (Table 3). The ¹³C NMR spectrum displayed 21 carbon signals, including a carbonyl (δ_C 180.3), 12 aromatic carbons (δ_C 93.0–162.6), a characteristic glucopyranosyl moiety (δ_C 100.4, 77.2, 76.4, 73.3, 69.7, and 60.7), and a hydroxyethyl group (δ_C 59.6 and 25.8). All these data suggested that **9** was a xanthone glycoside with a trisubstituted A-ring and a mono-substituted B-ring (Fernandes et al., 1998). The large coupling constant (*J* = 6.9 Hz) of the anomeric proton and acid hydrolysis result confirmed the sugar to be a β -D-glucopyranose. In the HMBC experiment of **9** (Fig. 5), the correlations from the hydrogen-bonded hydroxy proton at δ_H 13.10 to C-1 (δ_C 159.5), C-2 (δ_C 109.1), and C-9a (δ_C 103.1), from the methylene protons at δ_H 2.87 and 2.80 to C-1, C-2, and C-3 (δ_C 162.6), and from the anomeric proton at δ_H 5.05 to C-3 indicated the locations of the hydroxy, 2-hydroxyethyl, and glucopyranosyl group at C-1, C-2, and C-3 of A-ring, respectively. Additionally, the HMBC correlations from H-8 to C-4b (δ_C 149.2), C-6 (δ_C 124.9), and C-9 (δ_C

Table 3

¹H NMR (500 MHz) and ¹³C NMR (125 MHz) spectroscopic data for compounds **9**–**12** in DMSO-*d*₆.

Position	9		10		11		12	
	δ_C , tpye	δ_H , mult (<i>J</i> in Hz)	δ_C , tpye	δ_H , mult (<i>J</i> in Hz)	δ_C , tpye	δ_H , mult (<i>J</i> in Hz)	δ_C , tpye	δ_H , mult (<i>J</i> in Hz)
1	159.5, C		160.9, C		150.1, C		110.8, CH	7.75, d (3.0)
2	109.1, C		109.7, CH	6.78, d (8.3)	139.6, C		153.8	
3	162.6, C		136.6, CH	7.67, t (8.3)	125.4, CH	7.66, d (9.2)	125.5, CH	7.59, dd (9.2, 3.0)
4	93.0, CH	6.77, s	107.0, CH	7.03, d (8.3)	106.2, CH	7.06, d (9.2)	119.6, CH	7.67, d (9.2)
5	119.0, CH	7.53, d (9.0)	103.3, CH	7.31, s	146.4, C		118.2, CH	7.67, dd (8.7, 0.9)
6	124.9, CH	7.32, dd (9.0, 2.7)	153.0, C		121.0, CH	7.36, dd (7.9, 1.2)	135.5, CH	7.88, ddd (8.7, 8.0, 1.7)
7	154.0, C		144.6, C		124.1, CH	7.28, t (7.9)	124.3, CH	7.49, ddd (8.0, 8.0, 0.9)
8	107.9, CH	7.44, d (2.7)	108.2, CH	7.47, s	114.6, CH	7.60, dd (7.9, 1.2)	125.9, CH	8.20, dd (8.0, 1.7)
9	180.3, C		180.6, C		182.5, C		175.8, C	
9a	155.5, C		155.9, C		150.0, C		150.9, C	
4b	149.2, C		150.8, C		145.5, C		155.6, C	
8a	120.4, C		114.0, C		120.4, C		120.5, C	
9a	103.1, C		107.8, C		108.5, C		121.6, C	
10	25.8, CH ₂	2.80, m						
		2.87, m						
11	59.6, CH ₂	3.51, m						
1'	100.4, CH	5.05, d (6.9)	100.4, CH	5.14, d (7.1)	101.1, CH	4.94, d (6.9)	101.3, CH	4.97, d (7.4)
2'	73.3, CH	3.34, m	73.1, CH	3.37, m	73.3, CH	3.29, m	73.3, CH	3.29, m
3'	76.4, CH	3.31, m	76.0, CH	3.33, m	76.7, CH	3.31, m	76.4, CH	3.32, m
4'	69.7, CH	3.20, m	69.7, CH	3.20, m	69.7, CH	3.19, m	69.6, CH	3.21, m
5'	77.2, CH	3.48, m	77.3, CH	3.51, m	77.1, CH	3.36, m	77.1, CH	3.38, m
6'	60.7, CH ₂	3.47, m	60.7, CH ₂	3.49, m	60.7, CH ₂	3.47, dd (12.0, 5.9)	60.6, CH ₂	3.51, dd (11.9, 5.9)
		3.73, dd (10.2, 5.3)		3.74, dd (11.0, 5.7)		3.69, d (11.3)		3.71, dd (11.9, 5.4)
1-OH		13.10, s		12.80, s				
7-OH		10.06, s		9.55, s				
2'-OH		5.34, d (4.2)		5.39, d (3.9)		5.32, br s		5.39, d (4.6)
3'-OH		5.12, d (3.9)		5.14, d (4.7)		5.09, br s		5.10, d (3.7)
4'-OH		5.08, d (5.2)		5.10, d (5.3)		5.03, br s		5.03, d (5.2)
6'-OH		4.65, t (5.8)		4.66, t (5.7)		4.57, br s		4.59, t (5.4)
11-OH		4.60, t (5.5)						

180.3) and from H-6 to C-4b suggested that the non-chelated hydroxy group was attached to C-7 of B-ring. Therefore, the structure of **9** was assigned to be 1,7-dihydroxy-2-(2-hydroxyethyl)-3-*O*- β -D-glucopyranosylxanthone.

Hyperelatone F (**10**) was obtained as a yellow amorphous powder. Its HRESIMS showed a $[M + Na]^+$ peak at m/z 429.0787 (calcd for $C_{19}H_{18}NaO_{10}$, 429.0798), indicating a molecular formula of $C_{19}H_{18}O_{10}$ and 11 degrees of unsaturation. The 1H NMR data of **10** (Table 3) showed the character of a xanthone glycoside that exhibited two hydroxy groups [δ_H 12.80 (1H, s, 1-OH) and 9.55 (1H, s, 7-OH)], an ABM coupling system [δ_H 7.67 (1H, t, $J = 8.3$ Hz, H-3), 7.03 (1H, d, $J = 8.3$ Hz, H-4), and 6.78 (1H, d, $J = 8.3$ Hz, H-2)], two singlet aromatic protons [δ_H 7.47 (1H, s, H-8) and 7.31 (1H, s, H-5)], and an anomeric proton [δ_H 5.14 (1H, d, $J = 7.1$ Hz, H-1')]. The locations of two hydroxy groups and the sugar moiety were confirmed by 2D NMR experiments (Fig. 5). The HMBC correlations from the hydrogen-bonded hydroxy proton at δ_H 12.80 to C-1 (δ_C 160.9), C-2 (δ_C 109.7), and C-9a (δ_C 107.8) indicated that the hydroxy group was attached to C-1, which was supported by the 1H - 1H COSY correlations of H-2/H-3/H-4. The other hydroxy proton at δ_H 9.55 exhibited HMBC cross-peaks with C-6 (δ_C 153.0), C-7 (δ_C 144.6), and C-8 (δ_C 108.2), suggesting that the non-chelated hydroxy group was located at C-7. In addition, the HMBC correlation from the anomeric proton at δ_H 5.14 to C-6 indicated that the sugar moiety was linked at C-6. Analysis of the coupling constant of the anomeric proton and acid hydrolysis result confirmed the sugar unit to be a β -D-glucopyranose. The structure of **10** was thus determined to be 1,7-dihydroxy-6-*O*- β -D-glucopyranosylxanthone.

Hyperelatone G (**11**) has the same molecular formula of $C_{19}H_{18}O_{10}$ as **10** by analysis of HRESIMS (m/z 407.0978 [$M + H]^+$, calcd for $C_{19}H_{19}O_{10}$, 407.0978). IR and 1D NMR spectra revealed that these two compounds had the same functional groups. The 1H and ^{13}C NMR data of **11** (Table 3) are similar to those of the known compounds, 1,2,5-trihydroxyxanthone (Minami et al., 1994; Wu et al., 1998) and 1,5-dihydroxy-2-methoxyxanthone (Rath et al., 1996; Tala et al., 2015), except that a hydroxy group in 1,2,5-trihydroxyxanthone or the methoxy group in 1,5-dihydroxy-2-methoxyxanthone was replaced by a glucosyl moiety. This observation suggested that **11** was probably a 1,2,5-trisubstituted xanthone, which was further confirmed by the 1H - 1H COSY correlations of H-3 (δ_H 7.66)/H-4 (δ_H 7.06) and H-6 (δ_H 7.36)/H-7 (δ_H 7.28)/H-8 (δ_H 7.60) and the HMBC data (Fig. 5). Moreover, the HMBC correlation from the anomeric proton at δ_H 4.94 (H-1') to C-2 (δ_C 139.6) indicated that the glucosyl moiety was linked at C-2. Hence, the structure of **11** was determined to be 1,5-dihydroxy-2-*O*- β -D-glucopyranosylxanthone.

Hyperelatone H (**12**) has a molecular formula of $C_{19}H_{18}O_8$ deduced from HRESIMS peak at m/z 397.0899 [$M + Na]^+$ (calcd for $C_{19}H_{18}NaO_8$, 397.0899). Comprehensive analysis of the 1D NMR spectroscopic data (Table 3) strongly implied the presence of a mono-substituted xanthone and a sugar unit in **12**. The 1H NMR spectrum displayed seven aromatic proton resonances at δ_H 8.20 (1H, dd, $J = 8.0, 1.7$ Hz, H-8), 7.88 (1H, ddd, $J = 8.7, 8.0, 1.7$ Hz, H-6), 7.67 (1H, dd, $J = 8.7, 0.9$ Hz, H-5), 7.49 (1H, ddd, $J = 8.0, 8.0, 0.9$ Hz, H-7), 7.75 (1H, d, $J = 3.0$ Hz, H-1), 7.67 (1H, d, $J = 9.2$ Hz, H-4), and 7.59 (1H, dd, $J = 9.2, 3.0$ Hz, H-3) and one anomeric proton at δ_H 4.97 (1H, d, $J = 7.4$ Hz, H-1'). The ^{13}C NMR spectrum presented 19 carbon signals, including a carbonyl carbon (δ_C 175.8), 12 aromatic carbons (δ_C 110.8–155.6), and a sugar moiety (δ_C 101.3, 77.1, 76.4, 73.3, 69.6, and 60.6). The sugar moiety was characterized as a β -D-glucopyranose by the same method as described for **3**. The glycosidation position was located at C-2 (δ_C 153.8) based on a HMBC correlation from the anomeric proton (H-1') to C-2 and 1H - 1H COSY correlations of H-3/H-4 and H-5/H-6/H-7/H-8 (Fig. 5). Additionally, this assignment was confirmed by the downfield shift of C-2 and the upfield shifts of C-1, C-3, and C-4a in comparison with the chemical shifts for unsubstituted ring in xanthenes (Westerman et al., 1977; Fernandes et al., 1998). Thus, the structure of **12** was elucidated as 2-*O*- β -D-glucopyranosylxanthone.

Hyperelatone H (**12**) was only appeared as a synthetic product in 1929 (Robertson and Waters, 1929). Furthermore, there has been no NMR spectroscopic data reported for this compound by now. This is the first report of the occurrence of **12** as a natural product and its full NMR assignments based on the extensive 1D and 2D NMR experiments.

The remaining compounds were identified as cinchonain Ib (**5**) (Beltrame et al., 2006), cinchonain Ic (**6**) (Nonaka and Nishioka, 1982), (–)-epicatechin (**7**) (Davis et al., 1996), procyanidin B-2 (**8**) (Khan et al., 1997), tenuiside A (**13**) (Shi et al., 2013), 2,6-dimethoxy-*p*-hydroquinone 1-*O*- β -D-glucopyranoside (**14**) (Otsuka et al., 1989), eudionoside G (**15**) (Yamamoto et al., 2008), icariside B₂ (**16**) (Miyase et al., 1987), 2-phenylethyl- β -D-glucopyranoside (**17**) (Yoneda et al., 2008), and (*Z*)-3-hexenyl- β -D-glucopyranoside (**18**) (Mizutani et al., 1988) by comparison of their NMR data with the reported data in the literature. Among them, compounds **5**, **6**, **13**, and **15–18** were isolated from the genus *Hypericum* for the first time.

Moreover, the chemical profile of *H. elatoides* could provide chemotaxonomical information for verifying the systematic position of *H. elatoides* in the genus *Hypericum*. Based on morphological character analyses, *H. elatoides* was classified as either section *Roscyna* (Spach) R. Keller (Robson, 1977) or section *Ascyreia* Choisy (Robson, 2001). Molecular phylogenetic analyses showed that *H. elatoides* was closely related to *H. ascyron* L. (a member of section *Roscyna*), while section *Roscyna* nested with the large section *Ascyreia* (Meseguer et al., 2013; Nürk et al., 2013). Our results demonstrated that *H. elatoides* contained large amounts of flavonoids (Yan et al., 2018), flavanols derivatives (**4–8**), xanthenes (**9–13**), and phloroglucinol derivative (**1**), whereas several characteristic secondary metabolites such as hypericin, pseudohypericin, mangiferin, amentoflavone, and I3, II8-biapigenin, were not found in *H. elatoides*, which is most similar to the phytochemical profiles of the species from the sections *Ascyreia* and *Roscyna* (Kitanov and Nedialkov, 1998; Kitanov, 2001; Crockett and Robson, 2011; Camas et al., 2014; Cirak et al., 2016). The present study supports *H. elatoides* belonging to section *Roscyna* or *Ascyreia*, and possesses a potential taxonomic value for the infrageneric classification of the genus *Hypericum*.

Plants belonging to the genus *Hypericum* are well known for their therapeutic uses on neurological disorders (Rieli Mendes et al., 2002; Viana et al., 2005; Sarris, 2007; Grundmann et al., 2010). The best known species is *H. perforatum* L. (St. John's wort), which is widely used for the treatment of mild to moderate depression (Sarris, 2007; Kasper et al., 2010). Considering the fact that many previously isolated compounds from the genus *Hypericum* showed neuroprotective activities for antidepressant potential (Oliveira et al., 2016; Xu et al., 2016; Zhou et al., 2016), compounds **1–18** were evaluated for their protective effects against H_2O_2 -induced PC-12 cell injury, using captopril as a positive control. As shown in Table 4, compounds **2–7** and **11–13** exhibited neuroprotective activity, which significantly improved the survival rate of PC-12 cells in a dose-dependent manner. Among them, compounds **2–5**, **12**, and **13** were the most active, which may be due to the presence of hydroxy groups and their intrinsic molecular structures.

Recent studies support that neuroinflammation plays a crucial role in the development of depressive-like behaviors (Miller et al., 2009; Moylan et al., 2014). Inhibition of activated microglia-induced neuroinflammation might be an effective therapeutic target for depression (Catena-Dell'Osso et al., 2011; Réus et al., 2015; Dong et al., 2018). Therefore, all the isolated compounds were evaluated for their inhibitory effects on LPS-stimulated NO production in BV-2 microglial cells using Griess assay (Huang et al., 2015; Tang et al., 2018; Yan et al., 2018). Compounds **4**, **7**, **11–13**, and **18** showed significant inhibitory effects with IC₅₀ values of 5.83 ± 0.23 , 3.37 ± 0.13 , 3.84 ± 0.15 , 0.75 ± 0.02 , 1.39 ± 0.03 , and 2.95 ± 0.07 μ M, respectively, some of which exhibited stronger activity than the positive controls (Table 5). All the tested compounds did not show any significant cytotoxicity in BV-2 cells. Among the xanthone glucosides (**9–13**), compounds **11–13** showed much stronger activity than **9** and **10**, suggesting that the

Table 4
Neuroprotective effects of compounds 2–7 and 11–13 against H₂O₂-induced cell injury in PC-12 cells.

Compound ^a	Cell viability (% of control) ^b , concentration (μM)					
	0.3	1.0	3.0	10.0	30.0	100.0
Control	100.00 ± 2.63					
Model ^c	46.52 ± 0.56					
Captopril ^d	64.92 ± 0.15***	72.58 ± 0.15***	77.21 ± 0.71***	85.14 ± 0.41***	87.45 ± 0.11***	89.34 ± 0.15***
2	64.38 ± 3.99***	73.22 ± 2.52***	78.09 ± 2.39***	85.66 ± 0.24***	89.68 ± 0.19***	91.98 ± 0.26***
3	51.51 ± 1.49**	60.98 ± 0.73***	70.78 ± 0.02***	78.31 ± 0.11***	85.78 ± 0.80***	90.96 ± 0.41***
4	48.43 ± 0.63	59.80 ± 0.67**	70.72 ± 8.52**	73.31 ± 0.24***	82.00 ± 1.49***	84.74 ± 2.22***
5	49.70 ± 0.13**	61.19 ± 0.73***	71.30 ± 0.95***	73.60 ± 0.28***	81.65 ± 0.30***	84.10 ± 0.28***
6	47.87 ± 0.04	52.50 ± 5.13	54.70 ± 2.24*	66.00 ± 2.78***	77.47 ± 0.26***	83.86 ± 1.36***
7	47.61 ± 0.45	48.83 ± 0.80*	53.60 ± 0.26***	65.50 ± 1.06***	76.72 ± 0.37***	83.26 ± 0.09***
11	50.72 ± 0.37*	49.63 ± 0.13	55.53 ± 0.32***	64.63 ± 1.85***	75.00 ± 0.20***	80.20 ± 0.11***
12	63.17 ± 1.47***	69.62 ± 0.54***	76.95 ± 0.04***	82.71 ± 0.39***	87.27 ± 0.32***	90.08 ± 0.88***
13	52.09 ± 0.28**	65.72 ± 0.84***	68.45 ± 0.04***	75.43 ± 1.60***	82.55 ± 0.24***	85.12 ± 0.30***

P* < 0.05, *P* < 0.01, ****P* < 0.001 compared with model group.

^a Compounds 1, 8–10, and 14–18 showed weak activity at test concentrations.

^b Each value is expressed as mean ± SD from three independent experiments.

^c H₂O₂-only treatment group.

^d Positive control.

Table 5
Inhibitory effects of compounds 1–18 on LPS-induced NO production in BV-2 cells.

Compound	IC ₅₀ (μM) ^a	Compound	IC ₅₀ (μM) ^a
1	> 30	11	3.84 ± 0.15
2	> 30	12	0.75 ± 0.02
3	> 30	13	1.39 ± 0.03
4	5.83 ± 0.23	14	26.96 ± 1.07
5	> 30	15	> 30
6	> 30	16	> 30
7	3.37 ± 0.13	17	> 30
8	> 30	18	2.95 ± 0.07
9	> 30	Quercetin ^b	1.07 ± 0.04
10	> 30	Fluoxetine ^b	2.60 ± 0.06

^a Data are expressed as means ± SD based on three independent experiments.

^b Positive control.

presence of an *O*-glucosyl unit at C-2 or C-4 position of xantone, which might be related to a specific molecular geometry, could improve the inhibitory effect. Our results demonstrate that these novel phenolic metabolites from *H. elatoides* have neuroprotective or/and anti-neuroinflammatory activities and may be useful in the prevention and treatment of depression.

3. Conclusion

A previously undescribed PPAP, hyperelatone A (1), seven previously undescribed phenolic derivatives, hyperelatones B–H (2–4 and 9–12), together with ten known compounds (5–8 and 13–18) were isolated from the aerial parts of *H. elatoides*. The structures of these previously undescribed compounds were elucidated by spectroscopic methods, and their absolute configurations were determined using single-crystal X-ray diffraction crystallographic data, calculated and measured ECD data, and chemical evidence. The flavanone-resveratrol adducts (2 and 3) and phenylpropanoid-substituted flavan-3-ols (4–6) were isolated from *Hypericum* species for the first time. In addition, compounds 2–5, 12, and 13 showed potent neuroprotective activity against H₂O₂-induced cell injury in PC-12 cells at concentrations of 1.0–100.0 μM and 4, 7, 11–13, and 18 exhibited significant inhibitory effects on LPS-induced NO production in BV-2 cells. The present study will facilitate the development of new neuroprotective or/and anti-neuroinflammatory agents.

4. Experimental

4.1. General experimental procedures

Optical rotations were measured with an Auton Paar MCP300 automatic polarimeter (Anton Paar, Graz, Austria). ECD spectra were recorded with Applied Photophysics chirascan spectrometer (Applied Photophysics, Surrey, United Kingdom). The UV spectra were obtained on a Thermo Scientific Evolution-300 UV–visible spectrophotometer (Thermo Fisher Scientific, Waltham, MA, USA). The IR spectra were recorded on a Bruker Tensor 27 FT-IR spectrometer with KBr pellets (Bruker, Billerica, MA, USA). The NMR spectra were obtained on a Bruker Avance III 500 spectrometer (Bruker, Germany). HRESIMS were recorded on an AB Triple TOF[®] 4600 mass spectrometer (AB SCIEX, Redwood City, CA, USA). The X-ray crystallographic data was collected using a Bruker D8 Venture diffractometer with Mo K α radiation at 153 K (Bruker, Germany). Semi-preparative HPLC was performed on an Agilent 1100 series instrument equipped with a quaternary pump, a vacuum degasser, an autosampler, a diode array detector, and YMC Packed C₁₈ columns (5 μm, 250 × 10.0 mm and 150 × 4.6 mm, YMC Co., Ltd., Kyoto, Japan). Column chromatography was performed on silica gel (100–200 and 200–300 mesh, Qingdao Marine Chemical Ltd., Qingdao, China), reversed phase (RP)-C₁₈ resins (YMC Gel ODS-A-HG, 50 μm particle size, YMC Co., Ltd., Kyoto, Japan), and Sephadex LH-20 (Pharmacia Fine Chemicals, Uppsala, Sweden). Thin-layer chromatography was performed on silica gel 60 F₂₅₄ and RP-18 F_{254s} plates (Merck KGaA, Darmstadt, Germany).

4.2. Plant material

The aerial parts of *Hypericum elatoides* R. Keller (Hypericaceae) were collected in Dongjue Mountain, Qishan County, Shaanxi Province, China (latitude 34°34′–34°35′ North and longitude 107°45′–107°46′ East), in September 2016. The plant was identified by Professor Zai-Min Jiang, College of Life Sciences, Northwest A&F University. A voucher specimen (Jiang 1043) was deposited at the herbarium of Northwest A&F University (WUK), Yangling, China.

4.3. Extraction and isolation

The dried aerial parts (1.3 kg) of *H. elatoides* were cut into small pieces and extracted with MeOH (3 × 12 L) under reflux conditions (55 °C) for 8 h. After filtration and evaporation under reduced pressure, the obtained extract (334.8 g) was suspended in distilled water (3 L)

and partitioned successively with *n*-hexane (3 × 3 L), EtOAc (3 × 3 L), and *n*-BuOH (3 × 3 L). The *n*-hexane fraction (55.6 g) was fractionated by silica gel CC using a stepwise gradient of petroleum ether–Me₂CO (150:1 to 2:1) as eluents to afford eighteen fractions (H1–H18). Fr. H6 was subjected to silica gel CC and eluted with a gradient of *n*-hexane–Me₂CO (200:1 to 5:1) to give seven subfractions (H6.1–H6.7). Fr. H6.2 was further subjected to RP-C₁₈ CC (MeOH–Me₂CO, 2:1) followed by silica gel CC (*n*-hexane–Me₂CO, 300:1) to yield compound **1** (430.5 mg). The EtOAc fraction (49.2 g) was subjected to silica gel CC and eluted with a gradient of CH₂Cl₂–MeOH (100:1 to 2:1) to yield fifteen fractions (E1–E15). Fr. E9 was subjected to silica gel CC and eluted with a gradient of CHCl₃–MeOH–H₂O (15:1:0.05 to 4:1:0.1) to yield eight fractions (E9.1–E9.8). Fr. E9.4 was further separated by RP-C₁₈ CC (MeOH–H₂O, 1:2 to 1:1) to yield seven subfractions (E9.4.1–E9.4.7). Compound **17** (1.8 mg) was obtained from Fr. E9.4.3 by Sephadex LH-20 CC (MeOH–H₂O, 1:2). Compound **2** (23.6 mg) was obtained from Fr. E9.4.7 by RP-C₁₈ CC eluted first with MeOH–H₂O (1:1) and then with Me₂CO–H₂O (4:7). Fr. E9.5 was separated by RP-C₁₈ CC (Me₂CO–H₂O, 1:6 to 1:4) to give seven subfractions (E9.5.1–E9.5.7). Fr. E9.5.6 was subjected to RP-C₁₈ CC (MeOH–H₂O, 2:3) followed by RP-C₁₈ CC (Me₂CO–H₂O, 1:2) to provide compounds **5** (7.7 mg) and **6** (6.0 mg). Fr. E10 was separated by silica gel CC (CHCl₃–MeOH–H₂O, 15:1:0.05 to 3:1:0.1) to afford seven subfractions (E10.1–E10.7). Fr. E10.3 was further subjected to RP-C₁₈ CC (Me₂CO–H₂O, 1:5) to yield four fractions (E10.3.1–E10.3.4). Fr. E10.3.1 was further subjected to RP-C₁₈ CC (Me₂CO–H₂O, 1:6) to yield compound **7** (1341.4 mg). Fr. E10.3.2 was subjected to RP-C₁₈ CC (MeOH–H₂O, 2:5 to 2:3) to afford eight fractions (E10.3.2.1–E10.3.2.8). Compounds **4** (4.5 mg), **13** (7.0 mg), and **12** (9.1 mg) were obtained by the separations of Frs. E10.3.2.1, E10.3.2.3, and E10.3.2.7 on repeated RP-C₁₈ columns (MeOH–H₂O, 1:2), respectively. Fr. E10.3.4 was subjected to RP-C₁₈ CC (MeOH–H₂O, 2:3) followed by RP-C₁₈ CC (Me₂CO–H₂O, 1:2) to provide compound **10** (15.0 mg). Fr. E11 was subjected to silica gel CC and eluted with a gradient of CHCl₃–MeOH–H₂O (6:1:0.1 to 2:1:0.1) to afford six subfractions (E11.1–E11.6). Fr. E11.4 was further subjected to RP-C₁₈ CC (Me₂CO–H₂O, 1:2) to give compound **3** (233.3 mg). Fr. E11.5 was purified on a RP-C₁₈ column (MeOH–H₂O, 1:3) followed by a RP-C₁₈ column (Me₂CO–H₂O, 1:4) to yield compound **8** (33.7 mg). The *n*-BuOH fraction (71.0 g) was chromatographed over silica gel and eluted with a gradient of CH₂Cl₂–MeOH (20:1 to 1:1) to afford ten fractions (B1–B10). Fr. B1 was subjected to RP-C₁₈ CC (MeOH–H₂O, 1:6 to 1:1) to yield six fractions (B1.1–B1.6). Fr. B1.4 was further subjected to RP-C₁₈ CC (MeOH–H₂O, 1:5) to yield compound **16** (17.0 mg). Fr. B1.5 was purified on a RP-C₁₈ column (MeOH–H₂O, 2:5) to give compound **18** (20.1 mg). Fr. B2 was separated using RP-C₁₈ CC (MeOH–H₂O, 1:4) followed by RP-C₁₈ CC (Me₂CO–H₂O, 1:6) to yield compound **14** (18.4 mg). Fr. B3 was subjected to RP-C₁₈ CC and eluted with a gradient of MeOH–H₂O (1:4 to 1:1) to afford fourteen fractions (B3.1–B3.14). Fr. B3.6 was subjected to silica gel CC (CHCl₃–MeOH–H₂O, 5:1:0.1) followed by RP-C₁₈ CC (Me₂CO–H₂O, 1:4) to yield compound **15** (88.7 mg). Fr. B3.11 was separated by Sephadex LH-20 CC (MeOH–H₂O, 2:3) to yield compounds **9** (3.3 mg) and **11** (6.0 mg).

4.3.1. Hyperelatone A (**1**)

Colorless oil; $[\alpha]_D^{20} + 189.3$ (c 0.1, CHCl₃); UV (MeOH) λ_{\max} (log ϵ) 226 (3.9), 260 (2.4), 292 (2.0) nm; IR (KBr) ν_{\max} 3434, 1640 cm⁻¹; ¹H NMR (CDCl₃, 500 MHz) and ¹³C NMR data (CDCl₃, 125 MHz), see Table 1; HRESIMS (positive) m/z 517.3316 [M + H]⁺ (calcd for C₃₄H₄₅O₄, 517.3318).

4.3.2. Hyperelatone B (**2**)

Yellow amorphous powder; $[\alpha]_D^{20} + 56.8$ (c 0.05, MeOH); UV (MeOH) λ_{\max} (log ϵ) 215 (4.6), 291 (4.3) nm; IR (KBr) ν_{\max} 3405, 2931, 2842, 1635, 1463, 1362, 1268, 1167, 1024, 670 cm⁻¹; ECD (c = 0.1 mg/mL, MeOH) λ_{\max} ($\Delta\epsilon$) 228 (–11.4), 291 (+14.6), 316 (+5.2) nm; ¹H NMR (CD₃OD, 500 MHz) and ¹³C NMR data (CD₃OD, 125 MHz), see Table 2; HRESIMS (positive) m/z 521.1221 [M + Na]⁺

(calcd for C₂₉H₂₂NaO₈, 521.1212).

4.3.3. Hyperelatone C (**3**)

Yellow amorphous powder; $[\alpha]_D^{20} + 78.8$ (c 0.1, MeOH); UV (MeOH) λ_{\max} (log ϵ) 214 (4.5), 291 (4.2) nm; IR (KBr) ν_{\max} 3413, 2949, 2837, 1640, 1461, 1370, 1171, 1021, 668 cm⁻¹; ECD (c = 0.1 mg/mL, MeOH) λ_{\max} ($\Delta\epsilon$) 220 (–26.1), 291 (+31.2), 316 (+9.9) nm; ¹H NMR (CD₃OD, 500 MHz) and ¹³C NMR data (CD₃OD, 125 MHz), see Table 2; HRESIMS (positive) m/z 683.1760 [M + Na]⁺ (calcd for C₃₅H₃₂NaO₁₃, 683.1741).

4.3.4. Hyperelatone D (**4**)

Brown amorphous powder; $[\alpha]_D^{20} - 30.6$ (c 0.008, MeOH); UV (MeOH) λ_{\max} (log ϵ) 201 (4.6), 281 (3.7) nm; IR (KBr) ν_{\max} 3436, 2955, 2844, 1642, 1464, 1018, 664 cm⁻¹; ECD (c = 0.05 mg/mL, MeOH) λ_{\max} ($\Delta\epsilon$) 203 (15.8), 218 (–14.5), 254 (–6.0), 290 (–2.0) nm; ¹H NMR (CD₃OD, 500 MHz) and ¹³C NMR data (CD₃OD, 125 MHz), see Table 2; HRESIMS (positive) m/z 482.1209 [M – H₂O]⁺ (calcd for C₂₅H₂₂O₁₀, 482.1213).

4.3.5. Hyperelatone E (**9**)

Yellow amorphous powder; $[\alpha]_D^{20} - 15.2$ (c 0.05, MeOH); UV (MeOH) λ_{\max} (log ϵ) 238 (3.7), 261 (3.8) nm; IR (KBr) ν_{\max} 3414, 2927, 1706, 1520, 1384, 1222, 872 cm⁻¹; ¹H NMR (DMSO-*d*₆, 500 MHz) and ¹³C NMR data (DMSO-*d*₆, 125 MHz), see Table 3; HRESIMS (positive) m/z 451.1233 [M + H]⁺ (calcd for C₂₁H₂₃O₁₁, 451.1240).

4.3.6. Hyperelatone F (**10**)

Yellow amorphous powder; $[\alpha]_D^{20} - 9.6$ (c 0.1, MeOH); UV (MeOH) λ_{\max} (log ϵ) 252 (4.0) nm; IR (KBr) ν_{\max} 3431, 2942, 1639, 1475, 1280, 1224, 1027, 673 cm⁻¹; ¹H NMR (DMSO-*d*₆, 500 MHz) and ¹³C NMR data (DMSO-*d*₆, 125 MHz), see Table 3; HRESIMS (positive) m/z 429.0787 [M + Na]⁺ (calcd for C₁₉H₁₈NaO₁₀, 429.0798).

4.3.7. Hyperelatone G (**11**)

Yellow amorphous powder; $[\alpha]_D^{20} - 58.3$ (c 0.1, MeOH); UV (MeOH) λ_{\max} (log ϵ) 240 (4.1), 261 (4.2) nm; IR (KBr) ν_{\max} 3437, 1643, 1387, 1026, 771 cm⁻¹; ¹H NMR (DMSO-*d*₆, 500 MHz) and ¹³C NMR data (DMSO-*d*₆, 125 MHz), see Table 3; HRESIMS (positive) m/z 407.0978 [M + H]⁺ (calcd for C₁₉H₁₉O₁₀, 407.0978).

4.3.8. Hyperelatone H (**12**)

Yellow amorphous powder; $[\alpha]_D^{20} - 40.0$ (c 0.01, MeOH); UV (MeOH) λ_{\max} (log ϵ) 236 (4.1), 245 (4.1) nm; IR (KBr) ν_{\max} 3455, 2962, 1640, 1017, 668 cm⁻¹; ¹H NMR (DMSO-*d*₆, 500 MHz) and ¹³C NMR data (DMSO-*d*₆, 125 MHz), see Table 3; HRESIMS (positive) m/z 397.0899 [M + Na]⁺ (calcd for C₁₉H₁₈NaO₈, 397.0899).

4.4. Acid hydrolysis

The absolute configurations of the sugar moieties of **3** and **9–12** were determined by the acid hydrolysis method (Tanaka et al., 2007). Each compound (approximately 1.0 mg) was separately dissolved in 1 N HCl (0.5 mL), and then heated to 90 °C in a water bath for 2 h. After extraction with EtOAc two times, the H₂O-soluble fraction was evaporated to dryness under reduced pressure. The residue was dissolved in pyridine (0.1 mL) containing L-cysteine methyl ester hydrochloride (0.5 mg) and heated at 60 °C for 1 h. A 100 μ L solution of *o*-tolylisothiocyanate (0.5 mg) in pyridine was added and the reaction mixture was heated at 60 °C for 1 h. Then each reaction mixture was analyzed by the Waters 1525 HPLC system using a Waters 2489 UV/vis detector (at 250 nm). Analytical HPLC was performed on the YMC Packed C₁₈ column (5 μ m, 150 × 4.6 mm) with a linear gradient elution (CH₃CN–H₂O, 20:80 to 40:60) for 30 min. The derivative of D-glucose was identified in **3** and **9–12** by a comparison of the retention time with authentic D-glucose, which was subjected to the same derivatization

procedure.

4.5. Neuroprotective activity assay

PC-12 cells were purchased from the Cell Bank of Shanghai Institute of Biochemistry and Cell Biology, Chinese Academy of Sciences (Shanghai, China). PC-12 cells were cultured in DMEM/F12K supplemented with 10% FBS, penicillin G (100 U/mL), streptomycin (100 µg/mL), and sodium bicarbonate (2.5 g/L) at 37 °C in humidified atmosphere of 5% CO₂. The cells were plated in 96-well culture plates at a density of 1×10^5 cells/mL. After attachment, the cells were pretreated with varying concentrations (0.3, 1.0, 3.0, 10.0, 30.0, and 100.0 µM) of the test compounds for 24 h (or without drug, in the case of the model group) and exposed to 300 µM H₂O₂. After a 48 h treatment, the cell viability was measured using a CellTiter-Glo luminescent cell viability assay (Sasahara et al., 2013; Zhou et al., 2014; Zhang et al., 2016). The luminescence was recorded on a Biotek HM-1 microplate reader. Captopril was used as the positive control. The viability of the treated cells was expressed as a percentage of the nontreated control group.

4.6. Inhibition of NO production

BV-2 cells were purchased from Peking Union Medical College Cell Bank (Beijing, China) and cultured in DMEM supplemented with 10% FBS, penicillin G (100 U/mL), and streptomycin (100 µg/mL) at 37 °C in a humidified incubator with 5% CO₂. The NO concentration was detected by the Griess reagent (Beyotime Institute of Biotechnology, Shanghai, China). BV-2 cells were seeded at the density of 1.5×10^5 cells/mL in 96-well culture plates and treated individually with four different concentrations (0.3, 1.0, 3.0, and 10.0 µM) of tested compounds and LPS (1.0 µg/mL) for 24 h. After that, 50 µL of cell-free supernatant was allowed to react with an equal volume of Griess reagent for 15 min at room temperature in the dark. Then, the absorbance was measured at 550 nm using a microplate reader. Quercetin and fluoxetine were used as positive controls. The cell viability of the cultured cells was detected by MTT-based colorimetric method.

4.7. Statistical analysis

The data are expressed as means ± standard deviation (SD) of three replicate experiments. The significances of the intergroup differences were evaluated by one-way analysis of variance (ANOVA) followed by Dunnett's test using a computerized statistical package.

Conflicts of interest

There are no conflicts to declare.

Acknowledgments

This study was supported by the National Natural Science Foundation of China (No. 31800291), Natural Science Basic Research plan in Shaanxi Province (No. 2018JQ3032), the Fundamental Research Funds for the Central Universities (No. 2452017173), and Scientific Startup Foundation for Doctors of Northwest A&F University (No. 2452015356).

Appendix A. Supplementary data

Supplementary data related to this article can be found at <https://doi.org/10.1016/j.phytochem.2018.12.011>.

References

Abd El-Razek, M.H., 2007. NMR assignments of four catechin epimers. *Asian J. Chem.* 19, 4867–4872.

- Acuña, U.M., Figueroa, M., Kavalier, A., Jancovski, N., Basile, M.J., Kennelly, E.J., 2010. Benzophenones and biflavonoids from *Rheedia edulis*. *J. Nat. Prod.* 73, 1775–1779.
- Ayers, S., Zink, D.L., Brand, R., Pretorius, S., Stevenson, D., Singh, S.B., 2008. Struthiolanone: a flavanone-resveratrol adduct from *Struthiola argentea*. *Nat. Prod. Commun.* 3, 189–192.
- Beltrame, F.L., Filho, E.R., Barros, F.A.P., Cortez, D.A., Cass, Q.B., 2006. A validated higher-performance liquid chromatography method for quantification of cinchonain Ib in bark and phytopharmaceuticals of *Trichilia catigua* used as Catuaba. *J. Chromatogr. A* 1119, 257–263.
- Ben-Eliezer, D., Yechiam, E., 2016. *Hypericum perforatum* as a cognitive enhancer in rodents: a meta-analysis. *Sci. Rep.* 6, 35700.
- Bridi, H., Meirelles, G.C., von Poser, G.L., 2018. Structural diversity and biological activities of phloroglucinol derivatives from *Hypericum* species. *Phytochemistry* 155, 203–232.
- Camas, N., Radusiene, J., Ivanauskas, L., Jakstas, V., Kayikci, S., Cirak, C., 2014. Chemical composition of *Hypericum* species from the *Taeniocarpium* and *Drosanthe* sections. *Plant Systemat. Evol.* 300, 953–960.
- Catena-Dell'Osso, M., Bellantuono, C., Consoli, G., Baroni, S., Rotella, F., Marazziti, D., 2011. Inflammatory and neurodegenerative pathways in depression: a new avenue for antidepressant development? *Curr. Med. Chem.* 18, 245–255.
- Ciochina, R., Grossman, R.B., 2006. Polycyclic polyprenylated acylphloroglucinols. *Chem. Rev.* 106, 3963–3986.
- Cirak, C., Radusiene, J., Jakstas, V., Yayla, F., Seyis, F., Camas, N., 2016. Secondary metabolites of *Hypericum* species from the *Drosanthe* and *Olympia* sections. *S. Afr. J. Bot.* 104, 82–90.
- Crockett, S.L., Robson, N.K.B., 2011. Taxonomy and chemotaxonomy of the genus *Hypericum*. *Med. Aromat. Plant Sci. Biotechnol.* 5, 1–13.
- Davis, A.L., Cai, Y., Davies, A.P., Lewis, J.R., 1996. ¹H and ¹³C NMR assignments of some green tea polyphenols. *Magn. Reson. Chem.* 34, 887–890.
- Dong, S.Q., Zhang, Q.P., Zhu, J.X., Chen, M., Li, C.F., Liu, Q., Geng, D., Yi, L.T., 2018. Gypenosides reverses depressive behavior via inhibiting hippocampal neuroinflammation. *Biomed. Pharmacother.* 106, 1153–1160.
- Farag, M.A., Wessjohann, L.A., 2012. Metabolome classification of commercial *Hypericum perforatum* (St. John's wort) preparations via UPLC-qTOF-MS and chemometrics. *Planta Med.* 78, 488–496.
- Fernandes, E.G.R., Silva, A.M.S., Cavaleiro, J.A.S., Silva, F.M., Borges, M.F.M., Pinto, M.M.M., 1998. ¹H and ¹³C NMR spectroscopy of mono-, di-, tri- and tetrasubstituted xanthenes. *Magn. Reson. Chem.* 36, 305–309.
- Foo, L.Y., 1987. Phenylpropanoid derivatives of catechin, epicatechin and phylloflavan from *Phyllocladus trichomanoides*. *Phytochemistry* 26, 2825–2830.
- Gómez del Río, M.A., Sánchez-Reus, M.I., Iglesias, I., Pozo, M.A., García-Arencibia, M., Fernández-Ruiz, J., García-García, L., Delgado, M., Benedí, J., 2013. Neuroprotective properties of standardized extracts of *Hypericum perforatum* on rotenone model of Parkinson's disease. *CNS Neurol. Disord. - Drug Targets* 12, 665–679.
- Grundmann, O., Lv, Y., Kelber, O., Butterweck, V., 2010. Mechanism of St. John's wort extract (STW3-VI) during chronic restraint stress is mediated by the interrelationship of the immune, oxidative defense, and neuroendocrine system. *Neuropharmacology* 58, 767–773.
- Hamed, W., Brajeul, S., Mahuteau-Betzer, F., Thoison, O., Mons, S., Delpech, B., Nguyen, V.H., Sévenet, T., Marazano, C., 2006. Oblongifolins A–D, polyprenylated benzoylphloroglucinol derivatives from *Garcinia oblongifolia*. *J. Nat. Prod.* 69, 774–777.
- Huang, H.L., Lu, Z.Q., Chen, G.T., Zhang, J.Q., Wang, W., Yang, M., Guo, D.A., 2007. Phenylpropanoid-substituted catechins and epicatechins from *Smilax china*. *Helv. Chim. Acta* 90, 1751–1757.
- Huang, N., Rizshsky, L., Hauck, C., Nikolau, B.J., Murphy, P.A., Birt, D.F., 2011. Identification of anti-inflammatory constituents in *Hypericum perforatum* and *Hypericum gentianoides* extracts using RAW 264.7 mouse macrophages. *Phytochemistry* 72, 2015–2023.
- Huang, Z., Zhu, Z.X., Li, Y.T., Pang, D.R., Zheng, J., Zhang, Q., Zhao, Y.F., Ferreira, D., Zjawiony, J.K., Tu, P.F., Li, J., 2015. Anti-inflammatory labdane diterpenoids from *Leonurus macranthus*. *J. Nat. Prod.* 78, 2276–2285.
- Jamila, N., Khairuddean, M., Khan, S.N., Khan, N., 2014. Complete NMR assignments of bioactive rotameric (3→8) biflavonoids from the bark of *Garcinia hombroniensis*. *Magn. Reson. Chem.* 52, 345–352.
- Jat, L.R., 2013. Hyperforin: a potent anti-depressant natural drug. *Int. J. Pharm. Pharmaceut. Sci.* 5, 9–13.
- Kasper, S., Caraci, F., Forti, B., Drago, F., Aguglia, E., 2010. Efficacy and tolerability of *Hypericum* extract for the treatment of mild to moderate depression. *Eur. Neuropsychopharmacol.* 20, 747–765.
- Khan, M.L., Haslam, E., Williamson, M.P., 1997. Structure and conformation of the procyanidin B-2 dimer. *Magn. Reson. Chem.* 35, 854–858.
- Kitanov, G.M., Nedialkov, P.T., 1998. Mangiferin and isomangiferin in some *Hypericum* species. *Biochem. Syst. Ecol.* 26, 647–653.
- Kitanov, G.M., 2001. Hypericin and pseudohypericin in some *Hypericum* species. *Biochem. Syst. Ecol.* 29, 171–178.
- Lee, D., Park, E.J., Cuendet, M., Axelrod, F., Chavez, P.I., Fong, H.H.S., Pezzuto, J.M., Kinghorn, A.D., 2001. Cyclooxygenase-inhibitory and antioxidant constituents of the aerial parts of *Antirhea acutata*. *Bioorg. Med. Chem. Lett.* 11, 1565–1568.
- Meseguer, A.S., Aldasoro, J.J., Sanmartín, I., 2013. Bayesian inference of phylogeny, morphology and rang evolution reveals a complex evolutionary history in St. John's wort (*Hypericum*). *Mol. Phylogenet. Evol.* 67, 379–403.
- Miller, A.H., Maletic, V., Raison, C.L., 2009. Inflammation and its discontents: the role of cytokines in the pathophysiology of major depression. *Biol. Psychiatry* 65, 732–741.
- Minami, H., Kinoshita, M., Fukuyama, Y., Kodama, M., Yoshizawa, T., Sugiura, M., Nakagawa, K., Tago, H., 1994. Antioxidant xanthenes from *Garcinia subelliptica*. *Phytochemistry* 36, 501–506.

- Miyase, T., Ueno, A., Takizawa, N., Kobayashi, H., Karasawa, H., 1987. Studies on the glycosides of *Epimedium grandiflorum* Morr. var. *thunbergianum* (Miq.) Nakai. I. Chem. Pharm. Bull. 35, 1109–1117.
- Mizutani, K., Yuda, M., Tanaka, O., Saruwatari, Y., Fuwa, T., Jia, M., Ling, Y., Pu, X., 1988. Chemical studies on Chinese traditional medicine, dangshen. I. Isolation of (Z)-3- and (E)-2-hexenyl β -D-glucosides. Chem. Pharm. Bull. 36, 2689–2690.
- Moylan, S., Berk, M., Dean, O.M., Samuni, Y., Williams, L.J., O'Neil, A., Hayley, A.C., Pasco, J.A., Anderson, G., Jacka, F.N., Maes, M., 2014. Oxidative & nitrosative stress in depression: why so much stress? Neurosci. Biobehav. Rev. 45, 46–62.
- Nonaka, G., Nishioka, I., 1982. Tannins and related compounds. VII. Phenylpropanoid-substituted epicatechins, cinchonans from *Cinchona succirubra*. (1). Chem. Pharm. Bull. 30, 4268–4276.
- Nürk, N.M., Madriñán, S., Carine, M.A., Chase, M.W., Blattner, F.R., 2013. Molecular phylogenetics and morphological evolution of St. John's wort (*Hypericum*; Hypericaceae). Mol. Phylogenet. Evol. 66, 1–16.
- Oliveira, A.I., Pinho, C., Sarmiento, B., Dias, A.C.P., 2016. Neuroprotective activity of *Hypericum perforatum* and its major components. Front. Plant Sci. 7, 1004.
- Otsuka, H., Takeuchi, M., Inoshiri, S., Sato, T., Yamasaki, K., 1989. Phenolic compounds from *Coix lachryma-jobi* var. *Ma-yuen*. Phytochemistry 28, 883–886.
- Porzel, A., Farag, M.A., Mühlbradt, J., Wessjohann, L.A., 2014. Metabolite profiling and fingerprinting of *Hypericum* species: a comparison of MS and NMR metabolomics. Metabolomics 10, 574–588.
- Rath, G., Potterat, O., Mavi, S., Hostettmann, K., 1996. Xanthones from *Hypericum roeperianum*. Phytochemistry 43, 513–520.
- Réus, G.Z., Fries, G.R., Stertz, L., Badawy, M., Passos, I.C., Barichello, T., Kapczinski, F., Quevedo, J., 2015. The role of inflammation and microglial activation in the pathophysiology of psychiatric disorders. Neuroscience 300, 141–154.
- Rieli Mendes, F., Mattei, R., de Araújo Carlini, E.L., 2002. Activity of *Hypericum brasiliense* and *Hypericum cordatum* on the central nervous system in rodents. Fitoterapia 73, 462–471.
- Robertson, A., Waters, R.B., 1929. CCLXXXVIII. Synthesis of glucosides. Part III. Synthesis of glucosides of hydroxyxanthones. J. Chem. Soc. 0, 2239–2243.
- Robson, N.K.B., 1977. Studies in the genus *Hypericum* L. (Guttiferae): 1. Infrageneric classification. Bull. Br. Mus. Nat. Hist. (Bot.) 5, 291–355.
- Robson, N.K.B., 2001. Studies in the genus *Hypericum* L. (Guttiferae) 4 (1). Sections 7. *Roscyna* to 9. *Hypericum* sensu lato (part 1). Bull. Nat. Hist. Mus. Bot. 31, 37–88.
- Sarris, J., 2007. Herbal medicines in the treatment of psychiatric disorders: a systematic review. Phytoter. Res. 21, 703–716.
- Sasahara, H., Sugiyama, K., Tsukaguchi, M., Isogai, K., Toyama, A., Satoh, H., Saitoh, K., Nakagawa, Y., Takahashi, K., Tanaka, S., Onda, K., Hirano, T., 2013. Comparison of the pharmacological efficacies of immunosuppressive drugs evaluated by the ATP production and mitochondrial activity in human lymphocytes. Cell Med. 6, 39–45.
- Shi, T.X., Wang, S., Zeng, K.W., Tu, P.F., Jiang, Y., 2013. Inhibitory constituents from the aerial parts of *Polygala tenuifolia* on LPS-induced NO production in BV2 microglia cells. Bioorg. Med. Chem. Lett. 23, 5904–5908.
- Tala, M.F., Talontsi, F.M., Zeng, G.Z., Wabo, H.K., Tan, N.H., Spiteller, M., Tane, P., 2015. Antimicrobial and cytotoxic constituents from native Cameroonian medicinal plant *Hypericum riparium*. Fitoterapia 102, 149–155.
- Tanaka, N., Kashiwada, Y., Kim, S.Y., Sekiya, M., Ikeshiro, Y., Takaishi, Y., 2009. Xanthones from *Hypericum chinense* and their cytotoxicity evaluation. Phytochemistry 70, 1456–1461.
- Tanaka, T., Nakashima, T., Ueda, T., Tomii, K., Kouno, I., 2007. Facile discrimination of aldose enantiomers by reversed-phase HPLC. Chem. Pharm. Bull. 55, 899–901.
- Tang, D., Liu, L.L., He, Q.R., Yan, W., Li, D., Gao, J.M., 2018. Ansamycins with anti-proliferative and antineuroinflammatory activity from moss-soil-derived *Streptomyces cacaoi* subsp. *asoensis* H2S5. J. Nat. Prod. 81, 1984–1991.
- Tang, W., Hioki, H., Harada, K., Kubo, M., Fukuyama, Y., 2007. Antioxidant phenylpropanoid-substituted epicatechins from *Trichilia catigua*. J. Nat. Prod. 70, 2010–2013.
- Viana, A., do Rego, J.C., von Poser, G., Ferraz, A., Heckler, A.P., Costentin, J., Kuze Rates, S.M., 2005. The antidepressant-like effect of *Hypericum caprifoliatum* Cham & Schlecht (Guttiferae) on forced swimming test results from an inhibition of neuronal monoamine uptake. Neuropharmacology 49, 1042–1052.
- Vu, M., Herfindal, L., Juvik, O.J., Vedeler, A., Haavik, S., Fossen, T., 2016. Toxic aromatic compounds from fruits of *Nartheccium ossifragum* L. Phytochemistry 132, 76–85.
- Westerman, P.W., Gunasekera, S.P., Uvais, M., Sultanbawa, S., Kazlauskas, R., 1977. Carbon-13 NMR study of naturally occurring xanthones. Org. Magn. Reson. 9, 631–636.
- Wu, Q.L., Wang, S.P., Du, L.J., Yang, J.S., Xiao, P.G., 1998. Xanthones from *Hypericum japonicum* and *H. henryi*. Phytochemistry 49, 1395–1402.
- Xu, W.J., Li, R.J., Quasie, O., Yang, M.H., Kong, L.Y., Luo, J., 2016. Polyphenylated tetraoxygenated xanthones from the roots of *Hypericum monogynum* and their neuroprotective activities. J. Nat. Prod. 79, 1971–1981.
- Yamamoto, M., Akita, T., Koyama, Y., Sueyoshi, E., Matsunami, K., Otsuka, H., Shinzato, T., Takashima, A., Aramoto, M., Takeda, Y., 2008. Euodionosides A-G: megastigmene glucosides from leaves of *Euodia meliaeifolia*. Phytochemistry 69, 1586–1596.
- Yan, X.T., An, Z., Tang, D., Peng, G.R., Cao, C.Y., Xu, Y.Z., Li, C.H., Liu, P.L., Jiang, Z.M., Gao, J.M., 2018. Hyperelatosides A–E, biphenyl ether glycosides from *Hypericum elatoides*, with neurotrophic activity. RSC Adv. 8, 26646–26655.
- Yang, X.W., Grossman, R.B., Xu, G., 2018. Research progress of polycyclic polyphenylated acylphloroglucinols. Chem. Rev. 118, 3508–3558.
- Yang, X.W., Li, M.M., Liu, X., Ferreira, D., Ding, Y., Zhang, J.J., Liao, Y., Qin, H.B., Xu, G., 2015. Polycyclic polyphenylated acylphloroglucinol congeners possessing diverse structures from *Hypericum henryi*. J. Nat. Prod. 78, 885–895.
- Yoneda, Y., Krainz, K., Liebner, F., Potthast, A., Rosenau, T., Karakawa, M., Nakatsubo, F., 2008. “Furan endwise peeling” of celluloses: mechanistic studies and application perspectives of a novel reaction. Eur. J. Org. Chem. 2008, 475–484.
- Zhang, Q., Fan, D., Xiong, B., Kong, L., Zhu, X., 2013. Isolation of new flavan-3-ol and lignan glucoside from *Loropetalum chinense* and their antimicrobial activities. Fitoterapia 90, 228–232.
- Zhang, Y., Hu, X., Miao, X., Zhu, K., Cui, S., Meng, Q., Sun, J., Wang, T., 2016. MicroRNA-425-5p regulates chemoresistance in colorectal cancer cells via regulation of programmed cell death 10. J. Cell Mol. Med. 20, 360–369.
- Zhao, J., Liu, W., Wang, J.C., 2015. Recent advances regarding constituents and bioactivities of plants from the genus *Hypericum*. Chem. Biodivers. 12, 309–349.
- Zheleva-Dimitrova, D., Nedialkov, P., Momekov, G., 2013. Benzophenones from *Hypericum elegans* with antioxidant and acetylcholinesterase inhibitory potential. Pharmacogn. Mag. 9, S1–S5.
- Zhou, Z., Patel, M., Ng, N., Hsieh, M.H., Orth, A.P., Walker, J.R., Batalov, S., Harris, J.L., Liu, J., 2014. Identification of synthetic lethality of PRKDC in MYC-dependent human cancers by pooled shRNA screening. BMC Cancer 14, 944.
- Zhou, Z.B., Li, Z.R., Wang, X.B., Luo, J.G., Kong, L.Y., 2016. Polycyclic polyphenylated derivatives from *Hypericum uralum*: neuroprotective effects and antidepressant-like activity of uralodin A. J. Nat. Prod. 79, 1231–1240.